Carbohydrate Polymers 85 (2011) 325–333

Contents lists available at ScienceDirect

Carbohydrate Polymers

journal homepage: www.elsevier.com/locate/carbpol

Silk fibroin protein and chitosan polyelectrolyte complex porous scaffolds for tissue engineering applications

Nandana Bhardwaj, Subhas C. Kundu*

Department of Biotechnology, Indian Institute of Technology, Kharagpur 721302, India

ARTICLE INFO

Article history:
Received 22 September 2010
Received in revised form 28 January 2011
Accepted 15 February 2011
Available online 22 February 2011

Keywords:
Silk fibroin
Chitosan
Scaffolds
Biomaterials
Tissue engineering

ABSTRACT

In this study, we examined the porous polyelectrolyte complex scaffolds of silk fibroin and amino polysaccharide chitosan. The blended scaffolds were fabricated and characterized. The fabricated scaffolds showed pore sizes in the range of 100–160 μm as revealed by scanning electron microscope, good interconnectivity and high porosity. Fourier transform infrared and X-ray diffraction results demonstrated the blend formation. The addition of silk fibroin reduced the degradation of chitosan containing scaffolds in lysozyme solution. The blended scaffolds showed a higher compressive strength and modulus than the individual components. Chitosan incorporation had an antibacterial effect when incorporated at the higher levels in the blends. *In vitro* cytocompatibility results demonstrated that the blended scaffolds supported the growth and adhesion of feline fibroblasts. Taken together, the silk fibroin/chitosan scaffolds might be a promising biohybrid material for tissue engineering.

1. Introduction

There is a need to design effective biomaterials that can be utilized as tissue scaffolds/matrices for a variety of applications and also for the therapeutic reconstruction of damaged tissue. The three-dimensional biodegradable scaffolds take the role of extracellular matrix analogue, which serves as a necessary template or matrix for cell attachment (Alves da Silva et al., 2010; Meinel et al., 2004). This also provides physical support to guide the necessary differentiation and proliferation of cells into the targeted functional tissue or organ.

A number of natural and synthetic polymers such as collagen, gelatin, alginate, chitosan, silk fibroin, poly glycolic acid, hyaluronic acid are currently being employed as tissue engineering scaffolds for variety of applications (Altman et al., 2003; Garcia-Fuentes, Meinel, Hilbe, Meinel, & Merkle, 2009; Griffon, Sedighi, Schaeffer, Eurell, & Johnson, 2006; Hofmann et al., 2006; Cao & Kuboyama, 2010; Meinel et al., 2004). In the past few decades, the binary blends of polymers have received considerable attention from many researchers because it is a cost-effective way for preparing new materials with the desired physicochemical, thermal, mechanical properties, and/or biological responses. Blends with synthetic and natural polymers can imbibe the wide range of physicochemical properties and processing techniques for synthetic polymers as well as the biocompatibility and biological interactions of natural polymers.

Silk, as a unique family of proteins from silkworms and spiders, is a natural polymeric biomaterial with impressive oxygen and water vapour permeability, mechanical properties, biocompatibility and biodegradability (Mandal & Kundu, 2008; Omenetto & Kaplan, 2010). Silk is basically composed of two proteins, hydrophobic fibroin and hydrophilic sericin. Silk fibroin (SF) is the structural protein of fibers and sericins are the water-soluble glue-like proteins that bind the fibroin fibers together. Silk fibroin has been effectively used in many biomedical applications and is one of the most attractive biopolymers in both native fiber (Altman et al., 2003) and regenerated forms such as films (Hofmann et al., 2006), electrospun fibers (Bhardwaj & Kundu, 2010; Mandal & Kundu, 2010), wet-spun fibers (Liu et al., 2008), hydrogels (Dandu et al., 2009) and scaffolds (Mandal & Kundu, 2008; Meinel et al., 2004). For this reason SF has been successfully explored for the tissue engineering of bone, cartilage and ligaments (Cao & Kuboyama, 2010; Meinel et al., 2004; Wang, Blasioli, Kim, Kim, & Kaplan, 2006). SF is brittle on its own so blending with other polymers such as hyaluronic acid (Garcia-Fuentes et al., 2009), gelatin (Okhawilai, Rangkupan, Kanokpanont, & Damrongsakkul, 2010), poly (styrene), poly (ethylene oxide), collagen, alginate (Hardy & Scheibel, 2010), poly (vinyl alcohol) (Lee, Baek, Ki, & Park, 2007), sodium carboxymethyl cellulose (Kundu, Mohapatra, & Kundu, 2011), cellulose (Marsano, Corsini, Canetti, & Freddi, 2008) and others are employed for variety of tissue engineering applications.

Chitosan is a naturally derived polysaccharide, which is copolymer of β (1-4) linked *N*-acetyl-D-glucosamine and D-glucosamine

* Corresponding author. Tel.: +91 3222 283764; fax: +91 3222 278433.
E-mail address: kundu@hijli.iitkgp.ernet.in (S.C. Kundu).

0144-8617/$ – see front matter © 2011 Elsevier Ltd. All rights reserved.
doi:10.1016/j.carbpol.2011.02.027

units. It is soluble in dilute acids, where it carries a strong positive charge because of protonation of the amino group. Chitosan in different forms such as films, scaffolds, nanoparticles, microparticles, hydrogels has been used for variety of applications which include wound dressing (Khor & Lim, 2003), drug delivery systems (Han, Park, Hubbell, & Kim, 1998) and in tissue engineering applications such as for skin, bone, cartilage, etc. (Choi, Xie, & Xia, 2009; Griffon et al., 2006; Malafaya et al., 2005). Chitosan has inferior mechanical properties and very high swelling ability which causes it to get easily deformed. This is generally improved by blending with other polymers. Blends of chitosan with uncharged polymers such as poly (vinyl alcohol) (Tripathi, Mehrotra, & Dutta, 2009), polyesters (Alves da Silva et al., 2010), alginate (Han, Zhou, Yin, Yang, & Nie, 2010), hyaluronic acid (Yamane et al., 2005), hydroxyapatite (Thein-Han & Misra, 2009), gelatin (Jiankang et al., 2007) and other polyelectrolytes has been studied for numerous biomedical applications.

There are few reports of silk fibroin protein and chitosan blended scaffolds (Gobin, Froude, & Mathur, 2005; She et al., 2008) but some specific characterization and determination of other properties are still unexplored to implement these scaffolds for certain specific tissue engineering applications like cartilage. In order to use this blend for variety of applications such as cartilage, complete characterization of blended material is required. The polyelectrolyte complex scaffold of silk fibroin and chitosan formed via ionic interaction between carboxylate moieties on silk fibroin and protonated amines on chitosan is investigated in this present study. This study focuses mainly on understanding the effect of blending of silk fibroin and chitosan on morphology, stability, degradation, antimicrobial, mechanical properties and cell–matrix interactions.

2. Materials and methods

2.1. Materials

Bombyx mori silkworm fresh coccons were collected from Debra Sericulture Farm, West Midnapore, West Bengal, India. Chitosan was purchased from Sigma–Aldrich Chemicals (USA). The degree of deacetylation was 85%. Cell culture grade chemicals including Dulbecco's modified eagle medium (DMEM), fetal bovine serum, trypsin and penicillin–streptomycin antibiotics (Gibco BRL) and other chemicals used were of analytical grade.

2.2. Silk fibroin/chitosan solution formulation

Chitosan solution was prepared by dissolution in 2 wt% acetic acid and stirring for 6 h. The solution was centrifuged before use. Silk fibroin protein was isolated from *B. mori* silkworm coccons following a modification of standard extraction procedure (Sofia, McCarthy, Gronowicz, & Kaplan, 2001). SF and CS solutions each of 2% were used for blending. The SF/CS blend ratios 2:1, 1:1, 1:2 and 1:3 were prepared volumetrically and stirred for 15–20 min for uniform mixing.

2.3. Scaffold preparation and post processing

Scaffolds were prepared by freeze drying method. The pre freezing temperature used was −20 °C. If newly lyophilized SF/CS scaffolds were rehydrated in a neutral aqueous medium, they exhibited rapid swelling and ultimately dissolved, as a result of the residual acetic acid. In the current study, the scaffolds were neutralized by rehydrating in an ethanol series such as 100%, 70%, and 50% for 1 h, 30 min and 30 min each (Jiankang et al., 2007). After neutralization scaffolds were washed with PBS (pH 7.4) and followed by distilled water. The neutralized samples were lyophilized and subsequently used (Fig. 1).

2.4. Scanning electron microscopy (SEM)

Freeze-dried silk scaffolds were sectioned and were sputter coated with gold. The morphology of the scaffolds was observed with a JEOL-JSM 5800 SEM. Pore size of blended scaffolds was determined by Image J software (NIH, USA). For each type of scaffolds minimum 30 pores were examined.

2.5. Porosity

The porosity of the SF/CS scaffolds with different blending ratios was measured by liquid displacement method. The scaffolds were immersed in a known volume (V_1) of hexane in a graduated cylinder for 5 min. The total volume of hexane and the hexane impregnated scaffold was recorded as V_2. The hexane-impregnated scaffolds were then removed from the cylinder and the residual hexane volume was recorded as V_3. For all types of scaffolds experiments were carried out in triplicate.

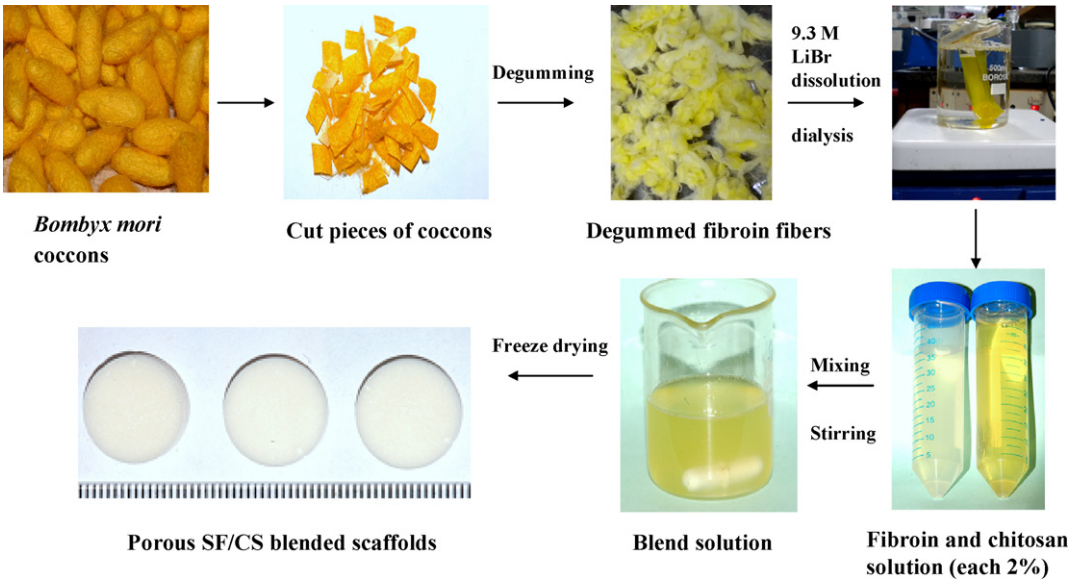

Fig. 1. Schematic illustration for fabricating silk fibroin (SF)/chitosan (CS) blended scaffolds.

The porosity of the scaffold ε was obtained by

$$\varepsilon(\%) = \frac{V_1 - V_3}{V_2 - V_3} \times 100$$

2.6. Fourier transform infra red (FTIR) spectroscopy

FTIR measurements were made using Thermo Nicolet-870 FTIR spectrophotometer in the spectral region 500–4000 cm^{-1}. For each measurement 32 interferograms were co-added and Fourier transformed at a resolution of 4 cm^{-1}. All samples were measured by the absorbance method. All spectra were recorded at room temperature and analyzed with Microcal Origin Version 6.0.

2.7. X-ray diffraction (XRD) analysis

High resolution XRD patterns were obtained using a X'pert PRO, PANalytical (3040/60) using CuKα radiation. The scanning speed was 0.0742°/s, and the measurements was done in the range of 2θ = 7–50° under 40 kV and 30 mA.

2.8. Evaluation of integral stability of the blended scaffolds

The integral stabilities of the constructs were evaluated by studying the *in vitro* release of the protein and carbohydrate from the constructs. The constructs were immersed in 10 mL ELIX water in triplicate and the protein and carbohydrate releases in water were estimated by the Bradford method and Anthrone assay respectively. The protein and carbohydrate releases were estimated over a period of time.

2.9. In vitro enzymatic degradation

Degradability of the chitosan and silk–chitosan scaffolds was determined by mass change of scaffolds after their incubation in 1 mL PBS (pH 7.4) containing 1.6 μg/mL of lysozyme (70,000 U/mg, Sigma) from egg white while shaking at 37 °C (Tangsadthakun, Kanokpanont, Sanchavanchavanalit, Banaprasert, & Damrongsakkul, 2006). After incubation for several time intervals, the scaffold was carefully withdrawn, repeatedly washed with PBS, and freeze-dried. The extent of the *in vitro* degradation was calculated as the percentage of weight difference of the dry scaffolds before and after hydrolysis with the lysozyme solution. The pH value of resultant PBS solution was also measured using pH meter.

2.10. Mechanical properties

The compressive mechanical properties of scaffolds were tested using a Universal Testing machine, Housfield-H25KS equipped with a 0.1 kN load cell at ambient room temperature using modification of ASTM method F451-95. The samples were presoaked in PBS for 2 h and were examined with crosshead speed 1 mm/min. At least three specimens were tested for each sample, and the averages and standard deviations are reported.

2.11. Antimicrobial properties

Antimicrobial properties of 3-D SF/CS blended scaffolds were determined by analysis of bacterial proliferation in suspension (Sarasam, Brown, Khajotia, Dmytryk, & Madihally, 2008). Gram positive bacteria *Staphylococcus aureus* (NCIM 2720) were used for determining antimicrobial properties. Here, samples were suspended in 5 mL of bacterial broth of known optical density (OD) taken in glass vials with rubber caps and incubated at 37 °C with constant, gentle shaking. Cultures without any scaffolds were taken as control. At various time points, 1 mL of each culture was retrieved and optical density was measured using a spectrophotometer at 600 nm. After 24 h, the matrices were removed and analyzed via SEM for bacterial adhesion.

2.12. In vitro cell culture

Cell viability and biocompatibility assessment were carried out using MTT assay. This assay is based on the reduction of tetrazole by living cells. Cleavage of the tetrazolium rings turns the pale yellow MTT [3-(4,5-dimethylthiazol-2-yl)-2,5-diphenyltetrasodium bromide] into dark blue formazan crystals, the concentration of which is directly proportional to the number of metabolically active cells. Therefore, the production of formazan can reflect the level of cell viability on the material. Silk fibroin, chitosan and blended scaffolds were presterilized and were conditioned in DMEM for 4 h before cell seeding. Equal number of cells (5×10^5) was seeded on each scaffold. In brief, total cells (5×10^5) were suspended in 30 μL medium and seeded. After 4 h of initial cell attachment, the seeded scaffolds were transferred to fresh culture plates containing medium. Fresh medium was replenished every alternate days and culture was incubated for 3 and 5 days in a humidified atmosphere containing 5% CO_2 at 37 °C. On specified days, cell viability was evaluated using MTT assay. In brief, 100 μL of MTT (5 mg/mL) diluted 1:10 times in PBS was added to each well followed by incubation for 4 h at 37 °C. After incubation, 0.5 mL of dimethyl sulfoxide was added to dissolve the blue formazan product formed and the absorbance was measured at 595 nm.

2.13. Statistical analysis

All data were reported as mean ± standard deviation. For each experiment N = 3–4 samples were used. One way analysis of variance (ANOVA) was performed to reveal differences among groups. Post hoc Tukey's test was carried out if variance was equal across groups. All statistical analyses were executed using SYSTAT 10.2 (Richmond, USA) and $p < 0.05$ was considered to be statistically significant.

3. Results and discussion

3.1. Scaffold preparation and microstructural (SEM) analysis

Morphology of silk, chitosan and SF/CS scaffolds, revealed by SEM photographs in Fig. 2A, indicates the porous structure with a three-dimensional interconnection throughout the scaffolds in all compositions. The interconnection of pores could still be observed after increasing the proportion of chitosan up to 67%. The pore size was in the range of 100–155 μm for the blended scaffolds as shown in Fig. 2A(b–d). Pure chitosan and silk fibroin showed pore size of 175 μm and 90 μm as observed in Fig. 2A(a and e) respectively. The blended SF/CS scaffolds showed higher pore sizes as compared to the pure silk fibroin. There was increase in the pore size with the increase of chitosan content in the blends. The blended scaffolds having high chitosan content show larger pore size as compared to silk fibroin scaffolds. This may be due to hydrophilicity of the chitosan.

3.2. Porosity measurement

Porosity measurement of scaffolds was done by liquid displacement method using hexane as a displacement liquid. Hexane was chosen because it permeates inside scaffolds without causing much shrinkage and swelling as compared to other liquids unlike ethanol, etc. Porosity determination is important in tissue engineering as highly porous structure provides much surface area that promotes better cell growth. All the scaffolds showed porosity

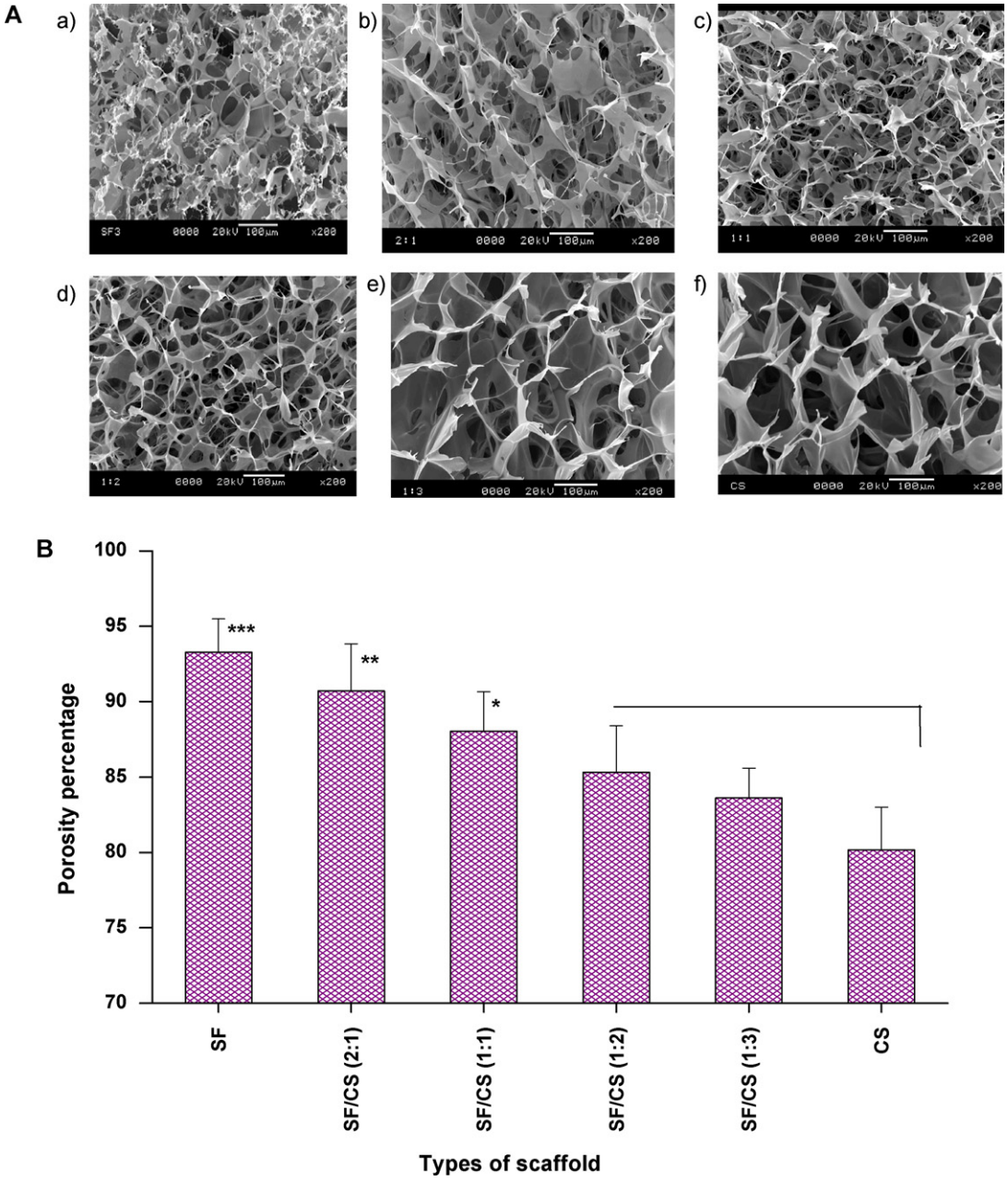

Fig. 2. (A) SEM pictographs of blended and pure silk and chitosan scaffolds. (a) Pure silk fibroin (2%, w/w), (b) SF/CS in 2:1, (c) SF/CS in 1:1, (d) SF/CS in 1:2, (e) SF/CS in 1:3 and (f) pure chitosan (2%, w/w). Scale bar = 100 μm. (B) Porosity percentage of blended and pure scaffolds. Each point represents the mean ± SD ($n = 3$). ***, **, and * show significant differences between groups at $p < 0.001$, $p < 0.01$ and $p < 0.05$ respectively.

ranging between 80 and 94% with maximum of 93.47% for pure silk fibroin scaffolds as shown in Fig. 2B. Among blends SF/CS (2:1) and (1:1) weight ratios showed significantly higher porosity as compared to other blends ($p < 0.01$) and that was more than 90%. As depicted in Fig. 2B, with the decrease of chitosan content, porosity of SF/CS scaffolds increases accordingly. The reason is obvious as with the decrease of chitosan content, the actual volume fraction occupied by the materials itself decreases.

3.3. FTIR spectroscopy and XRD analysis

FTIR spectra of fibroin/chitosan blended matrices with different compositions are shown in Fig. 3A. The silk fibroin film treated with ethanol showed absorption bands at 1625 (amide I), 1527 (amide II), and 1260 cm^{-1} (amide III) and 700 cm^{-1} (amide V), which were attributed to the β-sheet conformation of silk fibroin (Fig. 3A(f)) (Sampaio, Taddei, Monti, Buchert, & Freddi, 2005; She et al., 2008). On the other hand, the chitosan film showed absorption bands at 1173 and 900 cm^{-1}, which were attributed to the saccharide structure. Additionally bands at 1598 and 1651 cm^{-1} were attributed to the amino group of chitosan and the amide group of chitin respectively (Fig. 3A(a)) (Kweon et al., 2003). The double amide peaks for chitosan correspond to the partial *N*-deacetylation of chitin (Sugimoto, Morimoto, Sashiwa, Saimoto, & Shigemasa, 1998). The peaks at 1424 in chitosan scaffolds correspond to carboxyl (–COOH) stretching bands. A small but distinct change or shifting of the amide I band was observed in the SF/CS blend spectrum and it reached maximum with the SF/CS (2:1) blend ratio (Fig. 3A(e)) and the peak of the amino group (1173 cm^{-1}) was absent. The blended samples shown in Fig. 3A(b–e) exhibited the characteristic

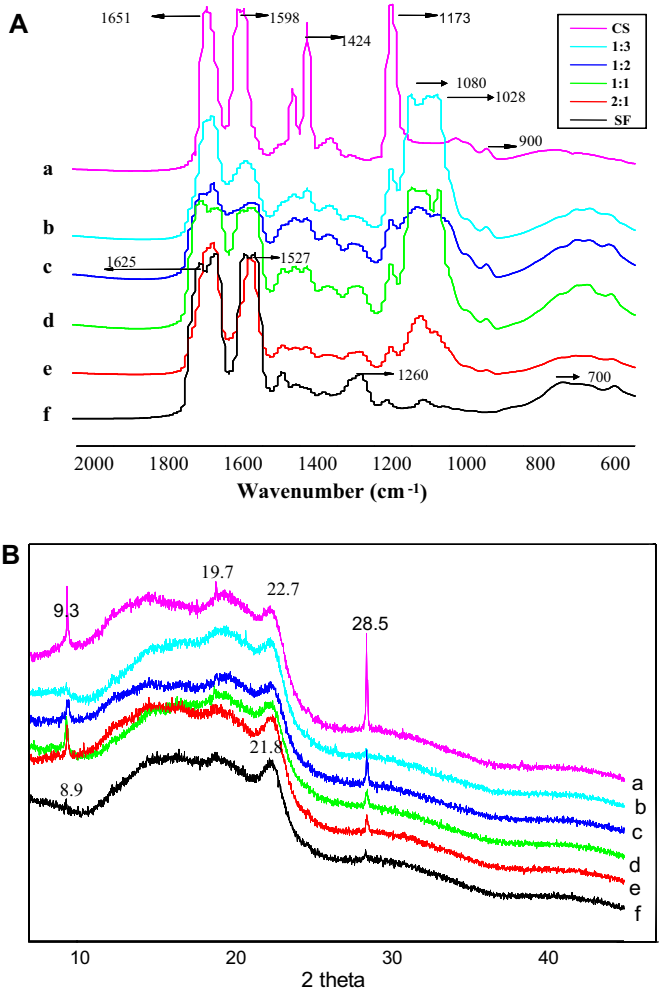

Fig. 3. (A and B) FTIR spectra and XRD diffraction peaks of pure and blended scaffolds. (a) Chitosan, (b) SF/CS (1:3), (c) SF/CS (1:2), (d) SF/CS (1:1), (e) SF/CS (2:1) and (f) pure silk.

absorption bands of both fibroin and chitosan with only intensity differences due to varying compositions of the two materials. SF/CS scaffolds showed additional bands at 1080 cm^{-1} and 1028 cm^{-1} that were not present in either chitosan or silk fibroin shows interaction of silk fibroin and chitosan.

To confirm the conformational changes, X-ray diffraction curves of SF/CS scaffolds were examined (Fig. 3B). Pure CS scaffold showed the broad peaks at 2θ 9.3, 19.7, and 22.7 respectively (Fig. 3B(a)), corresponding to the crystal-structure of the anhydrous form of chitosan (Ma et al., 2008). The XRD spectrum of chitosan (Fig. 3B(a)) has low crystallinity and the characteristic peaks at $2\theta = 9.3^\circ$ and 19.7° are assigned to crystal forms I and II (Fan, Chen, Yang, Lin, & Cao, 2009). Pure SF scaffold showed the peaks at $2\theta = 8.9$ and 21.8 respectively (Fig. 3B(f)), corresponding to the β-sheet crystalline structure (silk II) (Asakura, Tabeta, & Saito, 1985). This result indicates that the silk II crystalline structure exists in the fibroin sponge. SF/CS scaffolds shown in Fig. 3B(b–e) showed the characteristic peaks of both chitosan and silk fibroin suggesting presence of both in blend. The peaks at $2\theta = 28.5$ as shown in Fig. 3B(a–e), which do not exist in pure SF scaffolds were seen in SF/CS scaffolds and also in pure CS scaffolds. Furthermore, compared to pure SF scaffolds, these peaks show much stronger intensities, especially for the peak at $2\theta = 28.5$ and with the decrease of SF content, their intensities increase. This additional peak may be due to some remnants.

3.4. Evaluation of integral stabilities of constructs

This study was carried out to evaluate the stability of the blended matrices. If these matrices are to be utilized successfully, the two components, i.e. silk fibroin and chitosan, should be stable and should not leach out. Thus, *in vitro* protein and carbohydrate releases from blended SF/CS scaffolds were estimated using Bradford's reagent (Fig. 4A) and Anthrone reagent (Fig. 4B) respectively. Maximum protein release was observed in the case of SF/CS (2:1) blends while SF/CS (1:3) showed maximum carbohydrate release (Fig. 4B). With increase in the silk fibroin and chitosan contents, higher protein and carbohydrate releases were observed. It is possible that free fibroin molecules, which remain unblended in the blend, contribute most to the leached-out protein fraction and leaching was observed till 24 h. In contrast, maximum leaching of carbohydrate was observed till 48 h and after that there was not much change in the optical density. In addition, when compared to the total protein and carbohydrate needed for the fabrication of the constructs, the leached-out fraction is negligible, suggesting retention of bulk protein and carbohydrate within the blended scaffolds and contributes about 0.5–1.5% of the total (as estimated from standard curves).

3.5. In vitro degradation

In order to use the scaffolds for load bearing tissue engineering applications like bone, cartilage, there should be appropriate

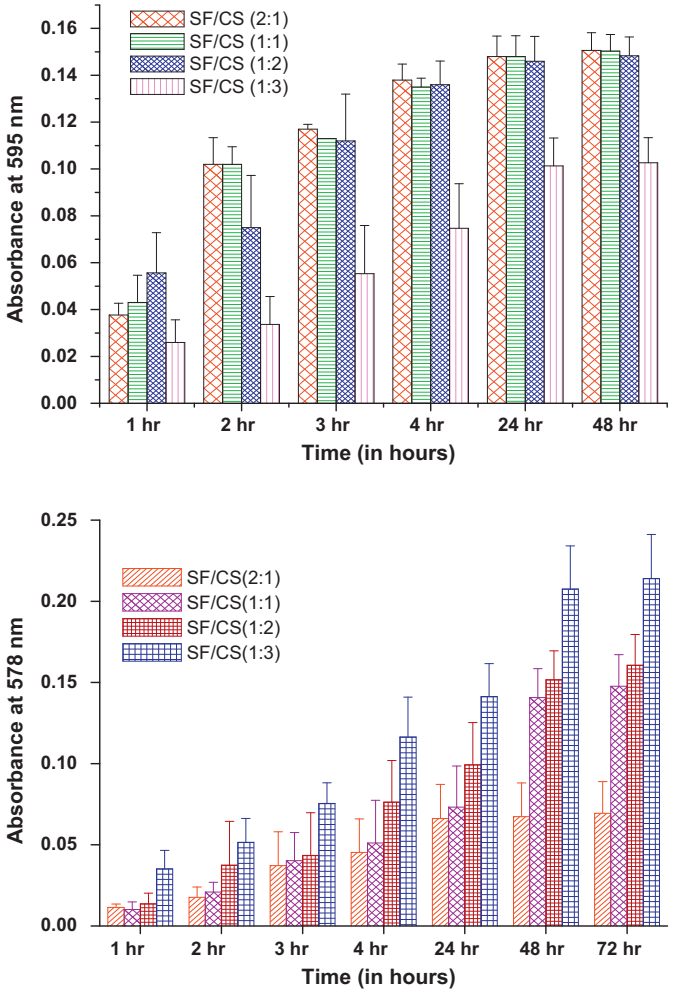

Fig. 4. *In vitro* release of protein (A) and carbohydrate (B) from blended scaffolds in water. Release was estimated over a time period (data represents mean ± SD, $n = 3$).

degradation rate. Chitosan degrades faster and its degradation rate depends on the degree of deacetylation. There is inverse relation between degradation rate and deacetylation degree (Kiang, Wen, Lim, & Leong, 2004). The higher the degree of deacetylation, the slower is the degradation. In this study 85% deacetylated chitosan is used to reduce the rate of degradation. Monitoring the weight-loss of scaffold and the changes in pH values of degradation media is employed in the present study. Lysozyme could hydrolyze the bindings between *N*-acetyl muramic acid and *N*-acetylglucosamine in the cell wall of bacteria. Therefore, this research uses lysozyme as degradation enzyme to investigate the time course of degradation of SF/CS 3-D porous scaffolds. The biodegradation results are shown in Fig. 5A and B. Chitosan scaffolds incubated in lysozyme had the highest weight reduction and were ~60% degraded after four weeks. The addition of silk fibroin reduced the degradation of scaffolds in lysozyme solution. When the proportion of chitosan was increased to 67% SF/CS (1:3), the remaining weights that sustained after 28 days were 50%. The scaffolds with more silk fibroin contents such as SF/CS (2:1) and SF/CS (1:1) showed only 30% loss in mass after 28 days with lysozyme and were significantly stable than chitosan scaffolds ($p < 0.001$) (Fig. 5A). This might be due to lack of active sites of lysozyme in blends. This suggests that the physical interaction between silk fibroin and chitosan possesses a greater steric hindrance effect to specific cleavage sites of lysozyme than that of the pure chitosan. Control scaffolds of each kind, which were kept in PBS (pH 7.4) without enzyme showed negligible or very less loss in mass after 28 days of incubation. The degradation rate of chitosan scaffolds is very fast; hence the addition of silk fibroin could prolong the biodegradability of scaffolds. The pH of the degradation solution was close to 7 even after 28 days of incubation (Fig. 5B). These results show that the degradation of the composite scaffold can be modified by changing the chitosan concentration or by addition of silk fibroin and there was not any formation of acidic by-products.

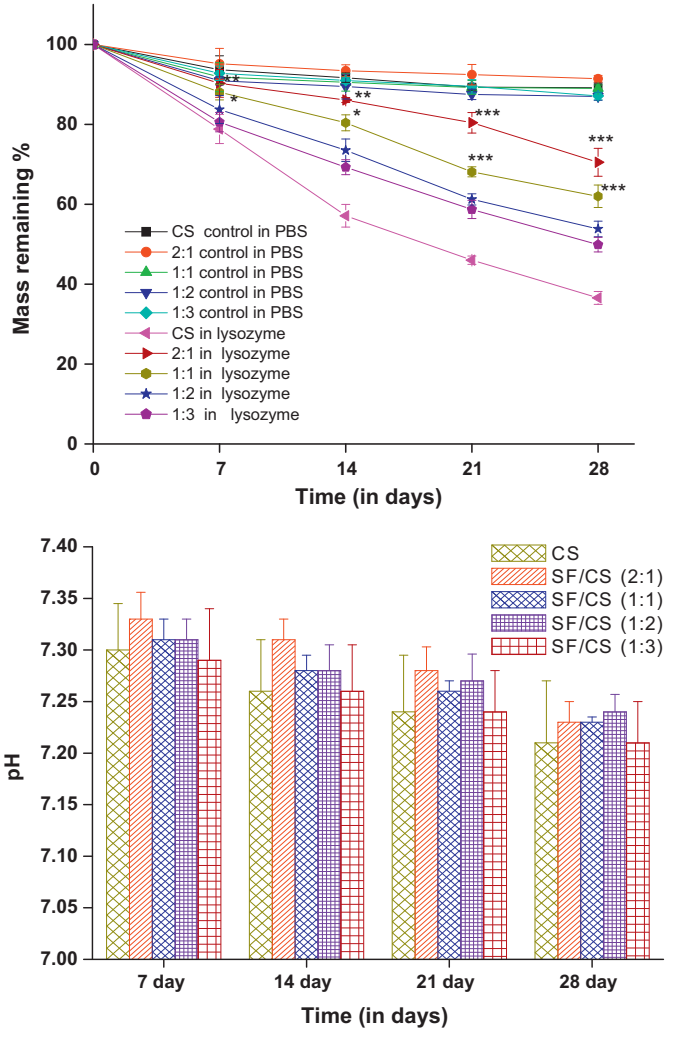

Fig. 5. (A and B) Degradation behavior and change in pH of the resultant solution of silk/chitosan (SF/CS) blended scaffolds in 0.05 M PBS containing 1.6 μg/mL of lysozyme and in pure PBS (pH 7.4) solution at 37 °C. Each point represents the mean ± SD ($n = 3$). ***, **, and * show significant differences between groups at $p < 0.001$, $p < 0.01$ and $p < 0.05$ respectively.

3.6. Mechanical strength determination

The compressive strength and modulus of SF/CS scaffolds are shown in Fig. 6A and B respectively. The compressive strength and modulus gradually decreased when the concentration of chitosan was increased. In this experiment scaffolds were compressed to 80%. The compressive strength of SF/CS (2:1) was maximum followed by SF/CS (1:1) and SF/CS (1:2) blended scaffolds. SF/CS (2:1) scaffolds showed 5-fold increase in compressive strength as compared to pure chitosan scaffolds ($p < 0.001$). Similar trend was observed for compressive modulus also. SF/CS (2:1) and SF/CS (1:1) showed significantly higher modulus as compared to pure silk fibroin and chitosan scaffolds. These results indicate that there

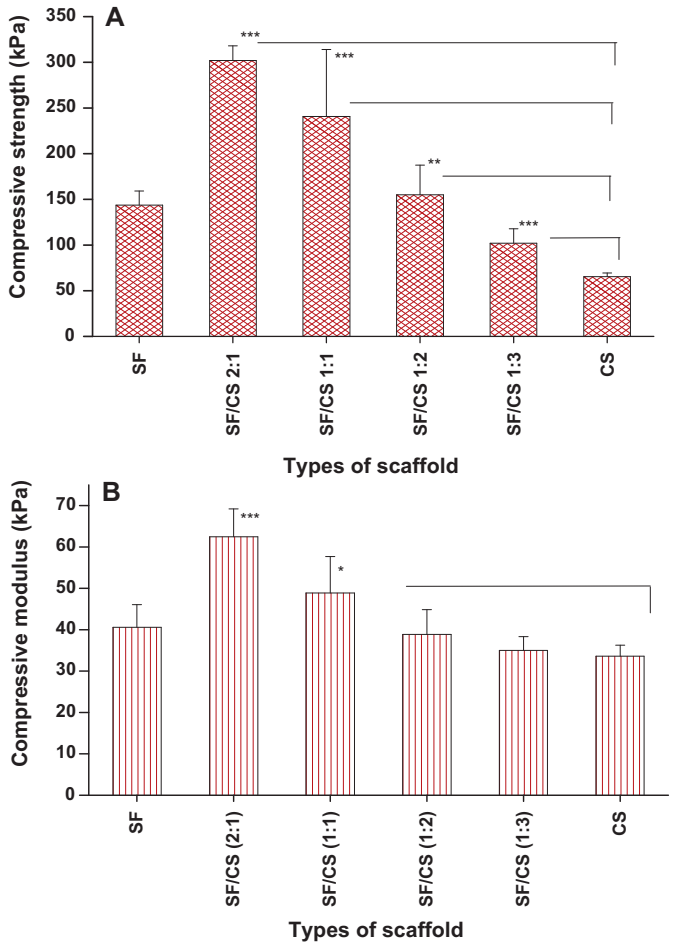

Fig. 6. (A and B) Compressive strength and modulus of SF/CS blended scaffolds. Scaffolds dimensions used are 10 mm thick and 13 mm in diameter. Each point represents the mean ± SD ($n = 3$). ***, ** and * show significant differences between groups at $p < 0.001$, $p < 0.01$ and $p < 0.05$ respectively.

is formation of compact structure due to ionic interaction, which probably leads to the increase in modulus and strength of blended scaffolds.

3.7. Antimicrobial properties

Antibacterial properties of blended scaffolds are studied as chitosan has intrinsic antimicrobial properties. The anti-microbial properties of chitosan are attributed to its cationic nature. The exact mechanism of the antimicrobial action of chitin, chitosan, and their derivatives is still unknown, but different mechanisms are proposed. The interaction between positively charged chitosan and negatively charged microbial cell wall leads to the leakage of proteinaceous and other intracellular constituents. The binding of chitosan with DNA and inhibition of mRNA synthesis occur via the penetration of chitosan into the nuclei of the microorganisms and interfering with the synthesis of mRNA and proteins (Raafat, von Bargen, Haas, & Sahl, 2008). Due to this antibacterial property chitosan is blended with other polymers in order to impart the antimicrobial ability (Rabea, Badawy, Stevens, Smagghe, & Steurbaut, 2003). We evaluated the effect of blending on bacterial cell–material interactions. Specifically, the bactericidal and prohibitive capacity of SF/CS blended scaffolds against bacterial proliferation and adhesion is studied. This study is conducted using oral pathogens *S. aureus* (Gram-positive, facultative anaerobe, spherical). *S. aureus* showed an initial increase in optical density (OD) for all matrices similar to the control (Fig. 7A). The control contained only bacterial cell suspension without any scaffolds. However, optical density of samples in suspension decreased from 6 h onwards and was significantly lower than those of control, pure silk fibroin and SF/CS (2:1) ($p < 0.01$) by 12 h, suggesting chitosan was potent against inhibition of *S. aureus* growth and was more

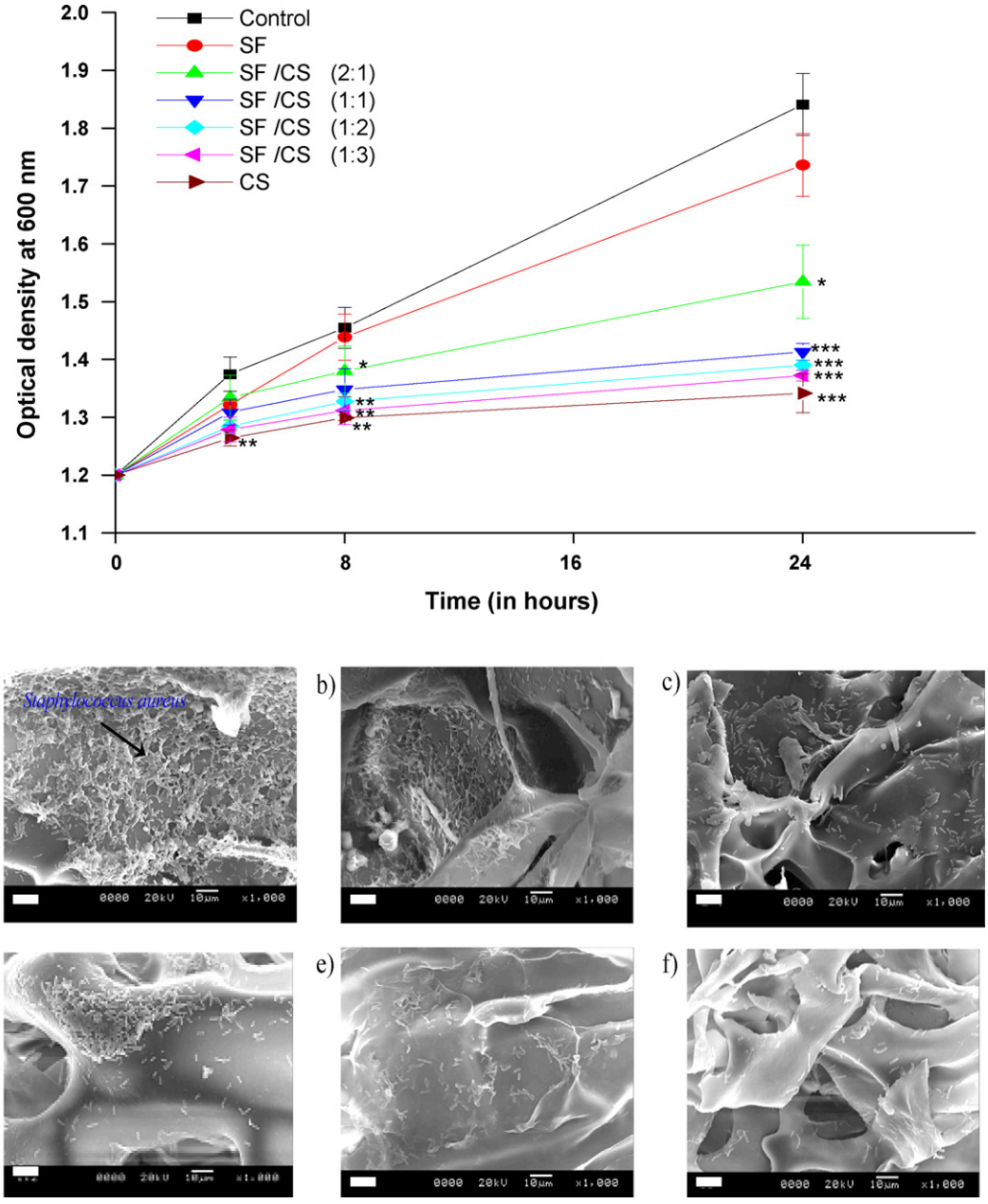

Fig. 7. (A) Influence of matrix architecture and composition on anti-bacterial activity of SFCS scaffolds. (B) Scanning electron micrographs showing adherence of *Staphylococcus aureus* on pure and blended scaffolds. Pure silk (fibroin (SF) scaffolds (a), SF/CS (2:1) (b), SF/CS (1:1) (c), SF/CS (1:2) (d), SF/CS (1:3) (e) and pure chitosan (CS) scaffolds (f). Each point represents the mean ± SD ($n = 3$). ***, **, and * show significant differences between groups at $p < 0.001$, $p < 0.01$ and $p < 0.05$ respectively. Scale bar = 10 μm.

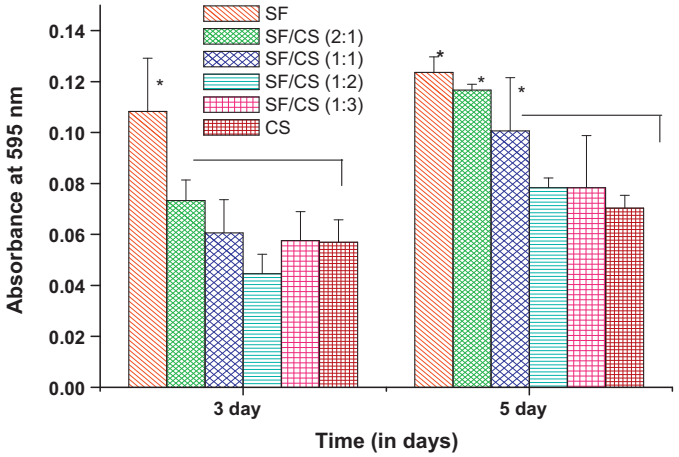

Fig. 8. Relative cell viability of AH927 on SF/CS scaffolds with different blending compositions after (a) 3 and (b) 5 days of cell seeding. Each point represents the mean ± SD ($n = 4$). *Significant differences between groups at $p < 0.05$ respectively.

effective as compared to blended scaffolds. There were no significant differences in the optical densities of the control, pure SF and SF/CS (2:1) sample suspensions ($p > 0.05$) after 24 h as compared to other blended and pure chitosan scaffolds. SF/CS (1:1), SF/CS (1:2) and SF/CS (1:3) showed significantly lower ($p < 0.001$) OD. SEM observation of all matrices after 24 h showed a similar trend (Fig. 7B). Chitosan and blended scaffolds with more chitosan content showed fewer adherences of *S. aureus* as compared to pure silk and SF/CS (2:1) scaffolds. Due to reduced oxygen tension in scaffolds, facultative anaerobic bacteria show greater antibacterial properties. With increase in silk content in blends, the antibacterial properties are compromised (Fig. 7A). Similar kinds of results are also observed with membranes and blended scaffolds of chitosan/PCL and of gliadins (Fernandez-Saiz, Lagaron, Hernandez-Munoz, & Ocio, 2008; Sarasam et al., 2008). In our study, there is less but growth of bacteria is observed in chitosan and in blended scaffolds, which have less silk fibroin content. This shows the bacteriostatic not bactericidal properties of the blended scaffolds.

3.8. Cell culture and biocompatibility of blended scaffolds

The cell viability and proliferation as a function of time on a scaffold are indicative of the cellular compatibility and appropriateness for tissue engineering applications (Han et al., 2010). Both silk fibroin and chitosan are reported for their good biocompatibility. The blended scaffolds particularly SF/CS (2:1) and SF/CS (1:1) showed good cell viability as pure silk fibroin scaffolds ($p > 0.05$) after 5 days (Fig. 8). The increased viability in blended scaffolds may be explained as interaction of positive amino groups of chitosan and negatively charged cells. The growth of feline fibroblast cells may be inhibited in the case of pure chitosan scaffolds by the extremely high affinity between cell and scaffold. This result suggests the suitability of this SF/CS scaffolds for tissue engineering applications and non-cytotoxic nature of the blends. Earlier reports (Altman, Gupta, Rios, Alt, & Mathur, 2010; She et al., 2008) of growth and attachment of hepatocytes and adipose tissue derived cells on these SF/CS scaffolds are in agreement with our results and confirm good cytocompatibility of feline fibroblasts.

4. Conclusions

A three-dimensional stable silk fibroin and chitosan (SF/CS) blended scaffolds are fabricated successfully with interconnected porous structure, suitable antimicrobial, degradation, and mechanical properties. The mechanical, degradation and biological properties of the scaffolds are significantly affected by changing the ratio of chitosan and silk fibroin in the scaffolds. These SF/CS blended scaffolds also facilitate the growth and attachment of feline fibroblast cells. Keeping in mind the good cytocompatibility and combined advantages of fibroin and chitosan, the blended scaffolds are promising candidates for various tissue engineering applications particularly for cartilage.

Acknowledgements

This work is financially supported by Department of Biotechnology (fellowship to Nandana Bhardwaj), Department of Science and Technology, Government of India and Indo-US Science and Technology Forum (IUSSTF), New Delhi.

References

Altman, G. H., Diaz, F., Jakuba, C., Calabro, T., Horan, R. L., Chen, J., et al. (2003). Silk-based biomaterials. *Biomaterials*, *24*, 401–416.
Altman, A. M., Gupta, V., Rios, C. N., Alt, E. U., & Mathur, A. B. (2010). Adhesion, migration and mechanics of human adipose-tissue-derived stem cells on silk fibroin–chitosan matrix. *Acta Biomaterialia*, *6*, 1388–1397.
Alves da Silva, M. L., Crawford, A., Mundy, J. M., Correlo, V. M., Sol, P., Bhattacharya, M., et al. (2010). Chitosan/polyester-based scaffolds for cartilage tissue engineering: Assessment of extracellular matrix formation. *Acta Biomaterialia*, *6*, 1149–1157.
Asakura, T., Tabeta, R., & Saito, H. (1985). Conformational characterization of *Bombyx mori* silk fibroin in the solid state by high-frequency carbon-13 cross polarization-magic angle spinning NMR, X-ray diffraction, and infrared spectroscopy. *Macromolecules*, *18*, 1841–1845.
Bhardwaj, N., & Kundu, S. C. (2010). Electrospinning: A fascinating fiber fabrication technique. *Biotechnology Advances*, *28*, 325–347.
Cao, H., & Kuboyama, N. (2010). A biodegradable porous composite scaffold of PGA/β-TCP for bone tissue engineering. *Bone*, *46*, 386–395.
Choi, S. W., Xie, J., & Xia, Y. (2009). Chitosan-based inverse opals: Three-dimensional scaffolds with uniform pore structures for cell culture. *Advanced Materials*, *21*, 2997–3001.
Dandu, R., Cresce, A. V., Briber, R., Dowell, P., Cappello, J., & Ghandehari, H. (2009). Silk–elastin like protein polymer hydrogels: Influence of monomer sequence on physicochemical properties. *Polymer*, *50*, 366–374.
Fan, J., Chen, J., Yang, L., Lin, H., & Cao, F. (2009). Preparation of dual-sensitive graft copolymer hydrogel based on N-maleoyl-chitosan and poly (N-isopropylacrylamide) by electron beam radiation. *Bulletin of Material Science*, *32*, 521–526.
Fernandez-Saiz, P., Lagaron, J. M., Hernandez-Munoz, P., & Ocio, M. J. (2008). Characterization of antimicrobial properties on the growth of *S. aureus* of novel renewable blends of gliadins and chitosan of interest in food packaging and coating applications. *International Journal of Food Microbiology*, *124*, 13–20.
Garcia-Fuentes, M., Meinel, A. J., Hilbe, M., Meinel, L., & Merkle, H. P. (2009). Silk fibroin/hyaluronan scaffolds for human mesenchymal stem cell culture in tissue engineering. *Biomaterials*, *30*, 5068–5076.
Gobin, A. S., Froude, V. E., & Mathur, A. B. (2005). Structural and mechanical characteristics of silk fibroin and chitosan blend scaffolds for tissue regeneration. *Journal of Biomedical Materials Research A*, *74A*, 465–473.
Griffon, D. J., Sedighi, M. R., Schaeffer, D. V., Eurell, J. A., & Johnson, A. L. (2006). Chitosan scaffolds: Interconnective pore size and cartilage engineering. *Acta Biomaterialia*, *2*, 313–320.
Han, D. K., Park, K. D., Hubbell, J. A., & Kim, Y. H. (1998). Surface characteristics and biocompatibility of lactide-based poly (ethylene glycol) scaffolds for tissue engineering. *Journal of Biomaterials Science: Polymer Edition*, *9*, 667–680.
Han, J., Zhou, Z., Yin, R., Yang, D., & Nie, J. (2010). Alginate–chitosan/hydroxyapatite polyelectrolyte complex porous scaffolds: Preparation and characterization. *International Journal of Biological Macromolecules*, *46*, 199–205.
Hardy, J. G., & Scheibel, T. R. (2010). Composite materials based on silk proteins. *Progress in Polymer Science*, *35*, 1093–1115.
Hofmann, S., Wong, C. T., Foo, P., Rossett, F., Textor, M., Vunjak-Novakovic, G., et al. (2006). Silk fibroin as an organic polymer for controlled drug delivery. *Journal of Controlled Release*, *111*, 219–227.
Jiankang, H., Dichen, L., Yaxiong, L., Bo, Y., Bingheng, L., & Qin, L. (2007). Fabrication and characterization of chitosan/gelatin porous scaffolds with predefined internal microstructures. *Polymer*, *48*, 4578–4588.
Khor, E., & Lim, L. Y. (2003). Implantable applications of chitin and chitosan. *Biomaterials*, *24*, 2339–2349.
Kiang, T., Wen, J., Lim, H. W., & Leong, K. W. K. W. (2004). The effect of the degree of chitosan deacetylation on the efficiency of gene transfection. *Biomaterials*, *25*, 5293–5301.
Kundu, J., Mohapatra, R., & Kundu, S. C. (2011). Silk fibroin/sodium carboxymethylcellulose blended films for biotechnological applications. *Journal of Biomaterials Science: Polymer Edition*, *22*, 519–539.

Kweon, H., Yoo, M. K., Park, I. K., Kim, T. H., Lee, H. C., Lee, H. S., et al. (2003). A novel degradable polycaprolactone networks for tissue engineering. *Biomaterials*, *24*, 801–808.

Lee, K. H., Baek, D. H., Ki, C. S., & Park, Y. H. (2007). Preparation and characterization of wet spun silk fibroin/poly (vinyl alcohol) blend filaments. *International Journal of Biological Macromolecules*, *41*, 168–172.

Liu, H., Xu, W., Zou, H., Ke, G., Li, W., & Ouyang, C. (2008). Feasibility of wet spinning of silk-inspired polyurethane elastic biofiber. *Materials Letters*, *62*, 1949–1952.

Ma, G., Yang, D., Zhou, Y., Xiao, M., Kennedy, J. F., & Nie, J. (2008). Preparation and characterization of water-soluble *N*-alkylated chitosan. *Carbohydrate Polymers*, *74*, 121–126.

Malafaya, P. B., Pedro, A. J., Peterbauer, A., Gabriel, C., Redl, H., & Reis, R. L. (2005). Chitosan particles agglomerated scaffolds for cartilage and osteochondral tissue engineering approaches with adipose tissue derived stem cells. *Journal of Materials Science: Materials in Medicine*, *16*, 1077–1085.

Mandal, B. B., & Kundu, S. C. (2008). Non-bioengineered silk fibroin protein 3D scaffolds for potential biotechnological and tissue engineering applications. *Macromolecular Bioscience*, *8*, 807–818.

Mandal, B. B., & Kundu, S. C. (2010). Biospinning by silkworms: Silk fiber matrices for tissue engineering applications. *Acta Biomaterialia*, *6*, 360–371.

Marsano, E., Corsini, P., Canetti, M., & Freddi, G. (2008). Regenerated cellulose–silk fibroin blends fibers. *International Journal of Biological Macromolecules*, *43*, 106–114.

Meinel, L., Hofmann, S., Karageorgiou, V., Zichner, L., Langer, R., Kaplan, D., et al. (2004). Engineering cartilage-like tissue using human mesenchymal stem cells and silk protein scaffolds. *Biotechnology and Bioengineering*, *88*, 379–391.

Okhawilai, M., Rangkupan, R., Kanokpanont, S., & Damrongsakkul, S. (2010). Preparation of Thai silk fibroin/gelatin electrospun fiber mats for controlled release applications. *International Journal of Biological Macromolecules*, *46*, 544–550.

Omenetto, F. G., & Kaplan, D. L. (2010). New opportunities for an ancient material. *Science*, *329*, 528–531.

Raafat, D., von Bargen, K., Haas, A., & Sahl, H. G. (2008). Insights into the mode of action of chitosan as an antibacterial compound. *Applied Environmental Microbiology*, *74*, 3764–3773.

Rabea, E. I., Badawy, M. E. T., Stevens, C. V., Smagghe, G., & Steurbaut, W. (2003). Chitosan as antimicrobial agent: Applications and mode of action. *Biomacromolecules*, *4*, 1457–1465.

Sampaio, S., Taddei, P., Monti, P., Buchert, J., & Freddi, G. (2005). Enzymatic grafting of chitosan onto *Bombyx mori* silk fibroin: Kinetic and IR vibrational studies. *Journal of Biotechnology*, *116*, 21–33.

Sarasam, A. R., Brown, P., Khajotia, S. S., Dmytryk, J. J., & Madihally, S. V. (2008). Antibacterial activity of chitosan-based matrices on oral pathogens. *Journal of Materials Science: Materials in Medicine*, *19*, 1083–1090.

She, Z., Jin, C., Huang, Z., Zhang, B., Feng, Q., & Xu, Y. (2008). Silk fibroin/chitosan scaffold: Preparation, characterization, and culture with HepG2 cell. *Journal of Materials Science: Materials in Medicine*, *19*, 3545–3553.

Sofia, S., McCarthy, M. B., Gronowicz, G., & Kaplan, D. L. (2001). Functionalized silk-based biomaterials for bone formation. *Journal of Biomedical Materials Research*, *54*, 139–148.

Sugimoto, M., Morimoto, M., Sashiwa, H., Saimoto, H., & Shigemasa, Y. (1998). Preparation and characterization of water soluble chitin and chitosan derivatives. *Carbohydrate Polymers*, *36*, 49–59.

Tangsadthakun, C., Kanokpanont, S., Sanchavanchavanalit, N., Banaprasert, T., & Damrongsakkul, S. (2006). Properties of collagen/chitosan scaffolds for skin tissue engineering. *Journal of Metals, Materials and Minerals*, *16*, 37–44.

Thein-Han, W. W., & Misra, R. D. K. (2009). Biomimetic chitosan–nanohydroxyapatite composite scaffolds for bone tissue engineering. *Acta Biomaterialia*, *5*, 1182–1197.

Tripathi, S., Mehrotra, G. K., & Dutta, P. K. (2009). Physicochemical and bioactivity of cross-linked chitosan–PVA film for food packaging applications. *International Journal of Biological Macromolecules*, *45*, 372–376.

Wang, Y., Blasioli, D. J., Kim, H. J., Kim, H. S., & Kaplan, D. L. (2006). Cartilage tissue engineering with silk scaffolds and human articular chondrocytes. *Biomaterials*, *27*, 4434–4442.

Yamane, S., Iwasaki, N., Majima, T., Funakoshi, T., Masuko, T., Harada, K., et al. (2005). Feasibility of chitosan-based hyaluronic acid hybrid biomaterial for a novel scaffold in cartilage tissue engineering. *Biomaterials*, *26*, 611–619.